Eur. Phys. J. Plus (2021) 136:463
https://doi.org/10.1140/epjp/s13360-021-01444-6

THE EUROPEAN PHYSICAL JOURNAL PLUS

Regular Article

Evaluation of thermal, electrical and magnetic properties of NiMnSnGd shape memory alloys by changing Gd amount for keeping the tin ratio constant

Ecem Öner, Mediha Kök[a]

Department of Physics, Faculty of Science, Firat University, Elaziğ, Turkey

Received: 5 January 2021 / Accepted: 16 April 2021

Abstract Heusler ferromagnetic shape memory alloys (FSMAs) have received significant attention due to their magnetocaloric effect. In this study, quaternary FSMAs based on NiMnSn alloyed with different amounts of Gd are investigated. The caloric, electrical and magnetic properties of the produced alloys are fully characterised. An increase in Gd alloying in the NiMnSn FSMAs results in a decrease in the characteristic temperatures. In addition, it is determined that the ratio of Mn and Ni is effective in changing the transformation temperature. The temperature-dependent electrical resistance measurements denote a sudden jump during the martensite phase transformation, while a decrease in the resistance value is observed during the austenite phase transformation. According to the magnetisation hysteresis, Gd significantly increases the magnetisation of the NiMnSn-based alloy.

1 Introduction

Smart materials are materials that respond to external physical (e.g. pressure, temperature, humidity, light and electric and magnetic fields), chemical (e.g. pH and solution) or biological stimuli by changing their counter quality and/or transforming energy [1–5]. Typical types of smart materials include piezoelectric materials, shape memory alloys (SMAs), magnetic shape memory alloys (MSMAs), magnetostrictive materials, electrostrictive materials, chromic materials and shape memory polymers [6–9].

Conventional SMAs exhibit both superelasticity and the shape memory effect (SME). While for superelasticity, the shape change occurs with the applied force, the shape change is observed with heating in the SME. Some of the conventional SMAs are NiTi, Cu-based, Fe-based, Co-based, Ni-based and Ti-based alloys [10]. There is considerable demand for NiTi alloys because they exhibit noticeable superelasticity and a strong SME [11–13]. MSMAs, unlike conventional SMAs, are expected to recover the original shape not only by applying force or temperature but also by using a magnetic field and reacting faster [14–17]. In recent years, MSMAs have received more attention due to their technological importance and physical properties and have been frequently studied by many researchers [18, 19].

[a] e-mail: msoglu@firat.edu.tr (corresponding author)

Published online: 28 April 2021

Ni-Mn-based Heusler alloys occupy an important place among magnetocaloric materials, since their structural phase transition is observed near room temperature and magnetic moments between two different phases of the material are rearranged. Recently, the demand for MSMAs that simultaneously display the SME and ferromagnetic behaviour has increased [20, 21]. Although Ni_2MnGa is the most used Heusler MSMA, Ni–Mn–Sn alloys are considered as alternative to Ni–Mn–Ga alloys. There are many alternatives to this combination, e.g. using Sn instead of Ga, which is preferred as it reduces costs and is promising for the future. Ni–Mn–Ga SMAs have low ductility and a martensitic phase transformation that have limited their application, where the weakness can be improved by substituting Ga with Sn [22]. For this reason, many studies have recently been conducted on the development of Ni–Mn–Sn-based alloys [18, 23–26].

Umetsu et al. observed that non-stoichiometric Ni–Mn–Z (Z = In, Sn or Sb) alloys differ from a traditional Ni–Mn–Ga ferromagnetic shape memory alloy, in which large magnetostriction occurs due to rearrangement of the magnetic variant [27, 28]. Kok et al. [29] added a high proportion of Cr into a Ni–Mn–Sn alloy. They found that Cr addition seriously affected on transformation temperature, crystal structure and magnetic properties of NiMnSn alloy. Ito et al. recently discovered an unusual type of ferromagnetic shape memory alloys (FSMAs) that indicates the martensitic transformation from the ferromagnetic parent phase to the anti-ferrous or paramagnetic martensite phase in the Ni–Mn–In, Ni–Co–Mn–In and Ni–Co–Mn–Sn Heusler alloy systems and confirmed the magnetic field-induced inverse martensitic transformation [30].

Rare-earth elements can operate at high temperature, and they are lightweight and have good wear and corrosion resistance. Moreover, they are also used as additive elements in MSMAs. For example, Sui et al. added small amounts of Gd into a NiMnGa alloy and this improved the two-way SME and thermomechanical properties of the alloy [31]. In another study, Cai and colleagues added Y to a NiMnGa alloy and found that the phase transformation temperature increased and the additive could improve the ductility of the alloy with compressive stress [32].

Gd is a moderately flexible, slightly hard, silvery-white rare-earth metal that is highly stable in air and has magnetocaloric properties. It is the only lanthanide that is ferromagnetic at near room temperature, with a Curie temperature of 293 K. Above this temperature, Gd is very strongly paramagnetic. As little as 1% Gd can increase the workability of iron and chromium alloys and their resistance to high temperatures and oxidation. Benefitting from this feature, it is also used in alloys to make magnets, electronic components and data storage discs. There are only limited studies regarding the Gd addition effect on NiMnSn SMAs, in which the mechanical, magnetic properties and change in the crystal structure of NiMnSnGd SMAs are investigated [33, 34].

In this study, Gd is chosen as a doping element in NiMnSn MSMAs because of its good magnetic properties and low curie temperature. The caloric electrical and magnetic properties of the quaternary alloys are investigated.

2 Experimental

Table 1 lists the appropriate ratios of high purity powders of Ni, Mn, Sn and Gd used to produce the NiMnSnGd alloys. First, the powders were mixed and then pelletised with a mechanical hydraulic compressor. The pelleted samples were melted using an arc melting furnace in a vacuum chamber and then the as-received alloys were homogenised at 900 °C for 24 h. The phase transformations were determined using a Perkin Elmer Sapphire Differ-

Table 1 The atomic percentage of NiMnSnGd alloys

Alloys' code	Ni	Mn	Sn	Gd
Gd0	50	38	12	–
Gd4	50	34	12	4
Gd6	50	32	12	6
Gd44	46	38	12	4
Gd66	44	38	12	6

ential Scanning Calorimetry (DSC) under a pure nitrogen atmosphere with a heating/cooling rate of 10 C°/min. For the analysis of the chemical composition and microstructure of the alloys, a Leo Evo-40 × VP scanning electron microscope equipped with energy-dispersive X-ray spectroscopy was used. The electrical resistivity against temperature was carried out for the samples using CRYO Industries of America Model No. REF-2261-202HT with a heating/cooling rate of 2 C°/min. Finally, the magnetisation of the produced alloys was determined using a Quantum Dizayn PPMS 7 (Physical Properties Measurement Systems) between -6 and 6 T at room temperature.

3 Result and discussion

Figure 1 shows the DSC curves of the Gd0, Gd4, Gd4, Gd6 and Gd66 samples, which were obtained at a heating/cooling rate of 10 K/min. The phase transformation temperatures (A_s, A_f, M_s and M_f) are listed in Table 2. The substitution of Ni with Gd generally reduced the transformation temperatures (TTs) of the NiMnSn alloy. The TTs were diminished by keeping the Mn constant and reducing Ni in the NiMnSnGd alloy (comparing Gd4 with Gd44, and Gd6 with G66). In different circumstances, the phase TTs dropped by keeping the Ni ratio constant. Thus, it can be stated that the change of other elements in addition to the Gd also affected the TTs.

Coll et al. [35] produced a MnNiSn alloy with a Mn ratio higher than the Ni ratio. They increased the weight percentage of Sn relative to Ni in three different compositions, whereby they found that the characteristic temperatures were reduced by decreasing the Ni composition. Likewise, the results were observed in the current study. Aydogdu et al. substituted Mn with B in a NiMnSn alloy and observed that the TTs increased with increasing B [36]. Similarly, Kök et al. [29] realised that the addition of Cr instead of Mn could increase the TTs of a NiMnSn alloy. Consequently, it can be noticed that Gd is a significant element that reduces the TTs of NiMnSn alloys. Gd is already preferred in magnetocaloric refrigerators because it is active at low temperatures [37]. In this study, we aimed to reduce the martensite TT of NiMnSn alloys to below room temperature and to enhance their magnetocaloric properties. The TTs fell to below 0 °C, indicating that the aim of this study had been achieved.

The enthalpy change refers to the energy required to transfer a solid–solid phase in an SMA. The enthalpy change values of NiMnSnGd alloys were obtained from the integration of the troughs and peaks of the martensitic phase transformation, based on the following equation [38–40]:

$$\Delta H^{M\to A} = \int_{A_s}^{A_f} \frac{\mathrm{d}q}{\mathrm{d}t}\left(\frac{\mathrm{d}T}{\mathrm{d}t}\right)^{-1}\mathrm{d}T. \tag{1}$$

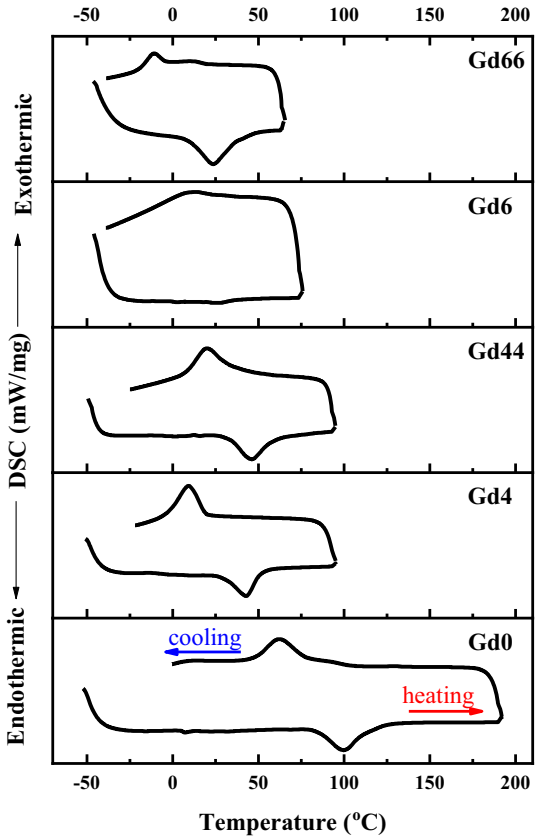

Fig. 1 The DSC results of NiMnSnGd alloys

Table 2 Phase transformation temperatures and enthalpy results of NiMnSnGd HTSMA

Samples	A_s (°C)	A_p (°C)	A_f (°C)	M_s (°C)	M_p (°C)	M_f (°C)	ΔH (J/g)	G_E (J/kg)
Gd0	84.9	100.7	123.4	89.3	61.3	42.7	10.35	1375.83
Gd4	29.4	42.5	58.9	21.7	9.1	− 8.1	7.50	846.54
Gd44	27.7	45.3	62.4	37.4	19.0	6.1	12.35	1483.09
Gd6	20.1	25.8	36.8	22.2	10.1	3.1	2.02	232.36
Gd66	5.10	22.7	44.7	− 2.8	− 11.7	− 17.6	5.51	236.64

Using the DSC software, the value of ΔH for the alloys was achieved and listed in Table 2. To compare, the alloys were divided into two different categories. In the first category, where the Gd ratio was constant (Gd4 and Gd44 alloys), the value of ΔH reduced by increasing the Mn/Ni ratio; a similar change was observed in Gd6 and Gd66 alloys. While the ΔH was decreased in the second category, where the Gd composition was increased in the alloy (Gd4-Gd6 and Gd44-Gd66). The DSC peak of the Gd6 was less sharp than other alloys. This result is in agreement with the elastic energy value (G_E) calculated by [39, 41, 42]:

$$G_E = \Delta G^{A\to M}(M_s) - \Delta G^{A\to M}\left(M_f\right) = \left(M_s - M_f\right)\Delta S^{M\to A} \tag{2}$$

where ΔG and ΔS are the Gibbs free energy and entropy changes of the martensitic phase transformations. The entropy change was calculated by [43, 44]:

$$\Delta S^{A(M)\rightarrow M(A)} = T_o \Delta H^{A(M)\rightarrow M(A)} \tag{3}$$

where T_o is the equilibrium temperature ($= \left(M_s + A_f\right)/2$) [45–47].

The compositional analysis of the alloys was accomplished with the mapping results obtained by EDS. Figure 2 shows the mapping results of the NiMnSn-based alloys. The distribution of the constituents changed with changing Mn and Ni ratios in the Gd6 and Gd66 alloys. Although Gd and Ni are almost homogeneous, the chemical changes between Mn and Sn are noticeable, e.g. the Mn ratio is higher in Gd66 than in Gd6. In the Gd6 alloy with less Mn content, secondary phases were more prominent and Mn-weighted precipitate phases were formed. Scanning electron microscopy (SEM) analysis was also performed to identify the microstructures and phases. The SEM analysis displays that the alloys provide both martensite and austenite phases. The reason for this is explained by the fact that the room temperature is between A_s and M_s temperatures, which is shown by the DSC measurements. Furthermore, the austenite phase provides more Mn compared to the martensite phase. Likewise, Saini et al. [48] obtained similar results for a $Ni_{46}Cu_4Mn_{45}Sn_5$ SMA. The SEM image was found to be a mixture of martensite and austenite phases. Furthermore, they stated that the needle-like component in the images represented the martensite phase, which is characteristic of the martensitic transformation.

Figure 3 shows the change of electrical resistance (ER) as a function of temperature for a complete thermal cycle. The ER measurements were performed for the Gd0, Gd44 and Gd66 alloys. Generally, the ER values of the martensite phase were higher than that of the austenite phase. In addition, it is indicated that the ER change with temperature for the martensitic phase transformation exhibits a semiconductor-like behaviour [49], i.e. more electron scattering is taken place with the formation of martensite variants. Moreover, the difference in crystal structure between the martensite phase and the austenite phase causes a change in the electron band structure of the shape memory alloys, which influences the electrical conductivity and electron scattering around the fermi energy level [50]. The increase in the Gd ratio caused reducing the hysteresis value of the NiMnSn SMA (ER resistance curves were obtained for Gd0, Gd44 and Gd66). Additionally, the electrical resistivity analysis of the martensite phase showed that the increase in the Gd ratio significantly increased the electrical resistivity.

Figure 4 shows the results of magnetisation of the NiMnSnGd alloys at room temperature. It is seen that none of those alloys attained saturation by applying a magnetic field of ± 6 T. However, none of the samples show magnetic hysteresis. Llamazares et al. [51] reported that there is a critical threshold (H_{cr}) of magnetic field for ternary Ni–Mn–Sn magnetic SMAs, where the magnetisation is completely reversible at field strengths below the H_{cr}. This property could be important for magnetic refrigerators. Since the hysteresis of all NiMnSnGd alloys is very narrow, they can be classified as soft magnetic behaviour SMAs. Heat treatment [51] and the measuring temperature [52] can also affect the magnetisation saturation.

The elements in an alloy provide information regarding the magnetic properties of MSMAs. There are three important elements in the NiMnSnGd alloy that affect the magnetisation, namely, Ni, Mn and Gd. The magnetic behaviour of materials results from the sum of the magnetic moments of the atoms. The magnetic moment value per atom is ~ 0.2–0.4 μ_B for Ni. For Mn, the element is ~ 2.84–4 μ_B and for Gd, the element is 6.8–8 μ_B [53, 54]. Accordingly, Gd is the most effective element with comparably high magnetisation. The M-H plots taken at room temperature show that the magnetisation value is raised by increasing the Gd ratio. Since the magnitude of magnetic moment per atom is Gd > Mn > Ni, so Mn

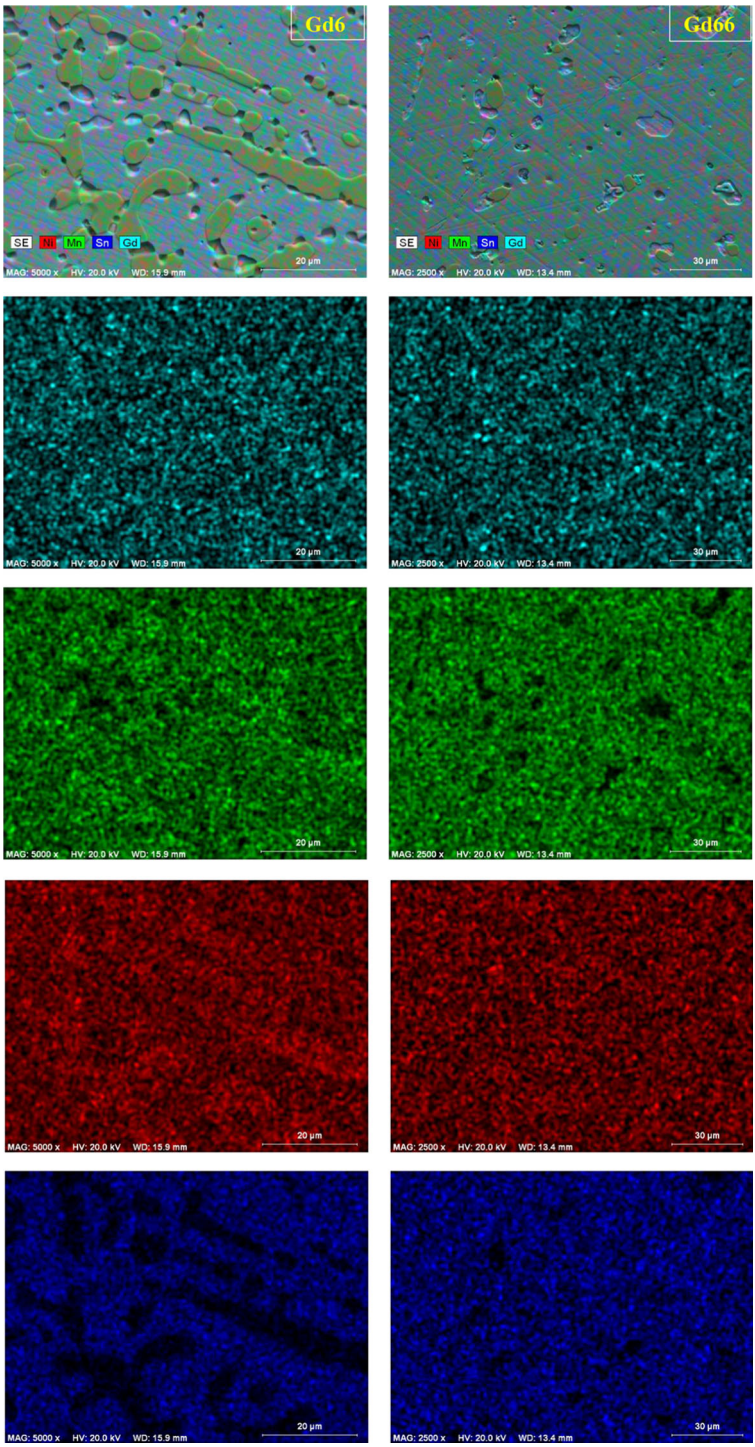

Fig. 2 The SEM images for the NiMnSnGd samples (the left- and right-side images are related to Gd6 and Gd66 alloys)

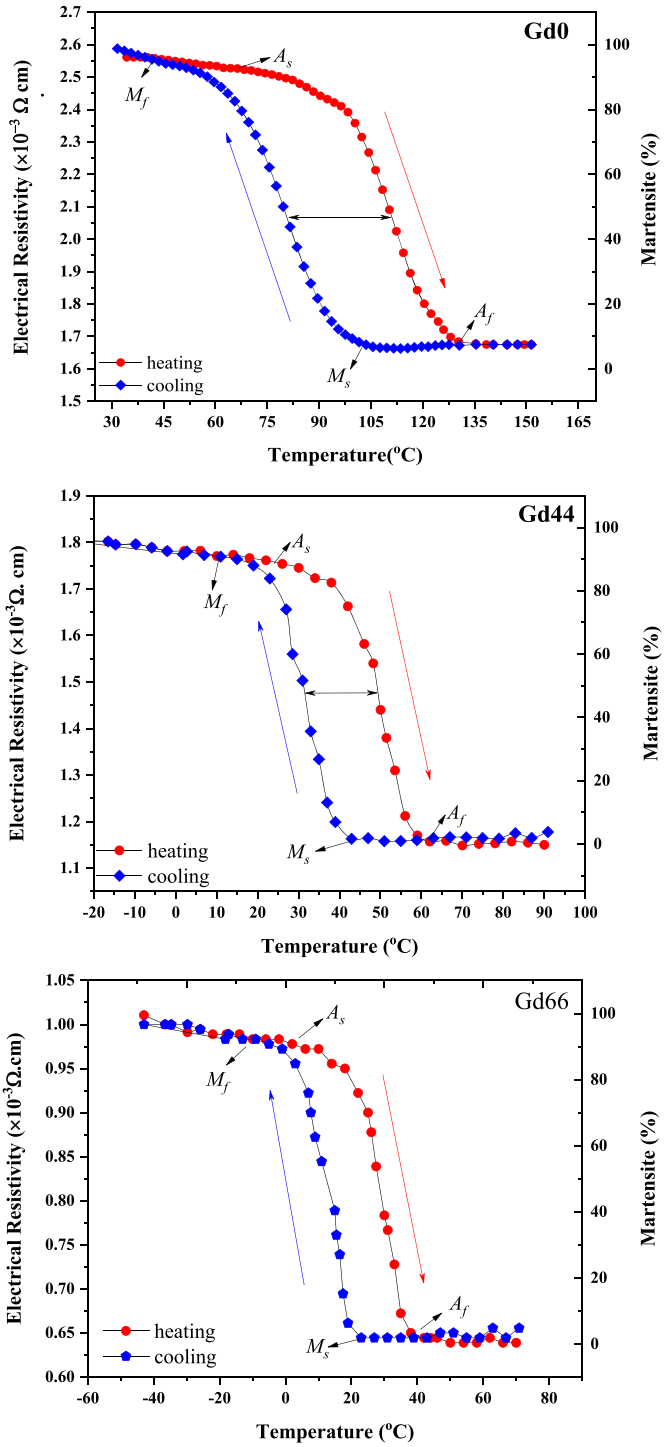

Fig. 3 Electrical resistivity graphs of Gd0, Gd44 and Gd66 samples by changing temperature

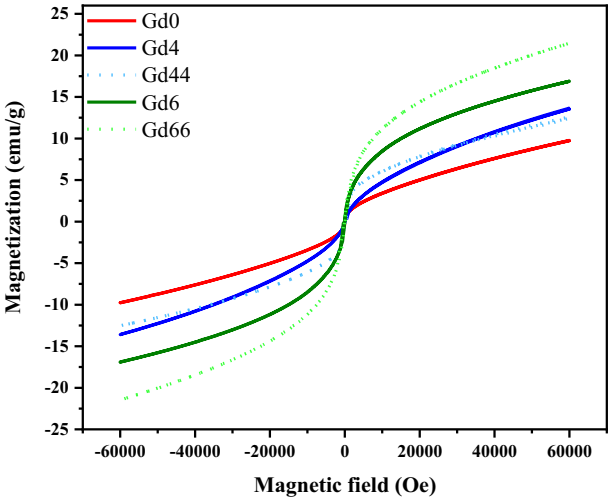

Fig. 4 Magnetisation curves of NiMnSn-Gd alloys at room temperature

has less effect on the magnetisation of the alloy compared to the Gd effect. Therefore, even though the Mn ratio is lower in Gd66 and Gd6 compared to other alloys, the atomic magnetic property of Gd has been more determinant.

4 Conclusions

In this study, Ni and Mn were substituted with a different ratio of Gd in Ni–Mn–Sn alloys. The caloric, electrical and magnetic properties of the alloy were investigated. The main outcomes can be summarised as follows:

- By fixing the Mn or Ni ratio in the alloy, increasing the Gd ratio reduced the TT values.
- The chemical and microstructure analysis showed that the NiMnSn-Gd alloy provided both martensite and austenite phases. The dominant phase was martensite with the friction of undissolved austenite phases. Additionally, it was found that the austenite contains more Mn compared to the martensite phase.
- It is known that SMAs exhibit a different crystal structure in the martensite and austenite phases. This change in crystal structure significantly affects the electron band structure of the alloy. Therefore, it was observed that the electrical resistance value of NiMnSnGd alloys increased in the martensite phase compared to the austenite phase. Furthermore, the hysteresis range of the NiMnSnGd alloy has decreased with the effect of Gd.
- It was observed that the magnetisation value of the NiMnSnGd alloy grew with an increasing Gd ratio. Because the atomic magnetic moment of Gd is higher than that of other alloying elements.

Acknowledgments This work was supported by the Management Unit of the Scientific Research Projects of Firat University (FUBAP) (Project Numbers: FF.20.14 and FF.20.06). This article is a part of the current Ph.D. study of Ecem Öner.

References

1. K. Otsuka, C.M. Wayman, *Shape Memory Materials* (Cambridge University Press, Cambridge, 1999).
2. P.O. Castillo-Villa, L. Mañosa, A. Planes, D.E. Soto-Parra, J.L. Sánchez-Llamazares, H. Flores-Zúñiga, C. Frontera, Elastocaloric and magnetocaloric effects in Ni–Mn–Sn (Cu) shape-memory alloy. J. Appl. Phys. **113**(5), 053506 (2013)
3. D.M. Addington, D.L. Schodek, *Smart Materials and New Technologies: For The Architecture and Design Professions* (Routledge, New York, 2005).
4. C. Wayman, Some applications of shape-memory alloys. JOM **32**(6), 129–137 (1980)
5. I.N. Qader, M. Kök, F. Dağdelen, Y. Aydogdu, A review of smart materials: researches and applications. El-Cezerî J. Sci. Eng. **6**(3), 755–788 (2019). https://doi.org/10.31202/ecjse.562177
6. S. Kamila, Introduction, classification and applications of smart materials: an overview. Am. J. Appl. Sci. **10**(8), 876 (2013)
7. T.W. Duerig, K. Melton, D. Stöckel, *Engineering Aspects of Shape Memory Alloys* (Butterworth-Heinemann, London, 2013).
8. D.C. Lagoudas, *Shape Memory Alloys: Modeling and Engineering Applications* (Springer, Berlin, 2008).
9. Z.D. Cırak, M. Kök, Investigation of the thermal and microstructural changes of CuAlNiNb quaternary shape memory alloys by different niobium amount. Eur. Phys. J. Plus **133**(7), 288 (2018)
10. Y. Ogawa, D. Ando, Y. Sutou, J. Koike, A lightweight shape-memory magnesium alloy. Science **353**(6297), 368–370 (2016)
11. W. Cai, X. Meng, L. Zhao, Recent development of TiNi-based shape memory alloys. Curr. Opin. Solid State Mater. Sci. **9**(6), 296–302 (2005)
12. K. Zhang, T. Ma, J. Liu, X. Tian, J. Zhu, C. Tan, Dynamically tunable and polarization-insensitive dual-band terahertz metamaterial absorber based on TiNi shape memory alloy films. Results Phys. 104001 (2021)
13. W. Zhao, E. Guo, K. Zhang, X. Tian, C. Tan, Martensite phase structure of Mg-Sc lightweight shape memory alloy and the effect of rare earth elements doping. Scr. Mater. **199**, 113863 (2021)
14. Y. Qu, D. Cong, S. Li, W. Gui, Z. Nie, M. Zhang, Y. Ren, Y. Wang, Simultaneously achieved large reversible elastocaloric and magnetocaloric effects and their coupling in a magnetic shape memory alloy. Acta Mater. **151**, 41–55 (2018)
15. V. Khovaylo, K. Skokov, O. Gutfleisch, H. Miki, T. Takagi, T. Kanomata, V. Koledov, V. Shavrov, G. Wang, E. Palacios, Peculiarities of the magnetocaloric properties in Ni-Mn-Sn ferromagnetic shape memory alloys. Phys. Rev. B **81**(21), 214406 (2010)
16. Z. Zhou, L. Yang, R. Li, J. Li, Q. Hu, J. Li, Martensite transformation, mechanical properties and shape memory effects of Ni–Mn–In–Mg shape memory alloys. Prog. Nat. Sci. Mater. Int. **28**(1), 60–65 (2018)
17. V.D. Buchel'nikov, A.N. Vasiliev, V. Koledov, S.V.E. Taskaev, V.V.E. Khovaylo, V.G.E. Shavrov, Magnetic shape-memory alloys: phase transitions and functional properties. Phys. Usp. **49**(8), 871–877 (2006)
18. A. Planes, L. Mañosa, M. Acet, Magnetocaloric effect and its relation to shape-memory properties in ferromagnetic Heusler alloys. J. Phys. Condens. Matter **21**(23), 233201 (2009)
19. H.D. Chopra, C. Ji, V. Kokorin, Magnetic-field-induced twin boundary motion in magnetic shape-memory alloys. Phys. Rev. B **61**(22), R14913 (2000)
20. E. Stern-Taulats, P.O. Castillo-Villa, L. Mañosa, C. Frontera, S. Pramanick, S. Majumdar, A. Planes, Magnetocaloric effect in the low hysteresis Ni–Mn–In metamagnetic shape-memory Heusler alloy. J. Appl. Phys. **115**(17), 173907 (2014)
21. P. Czaja, W. Maziarz, J. Dutkiewicz, Microstructure evolution and its influence on martensitic transformation in Ni–Mn–Sn alloys. Inżynieria Materiałowa **34**(3), 149–152 (2013)
22. V. Chernenko, C. Segui, E. Cesari, J. Pons, V. Kokorin, Sequence of martensitic transformations in Ni–Mn–Ga alloys. Phys. Rev. B **57**(5), 2659 (1998)
23. S.J. Murray, M. Marioni, S. Allen, R. O'handley, T.A. Lograsso, 6% magnetic-field-induced strain by twin-boundary motion in ferromagnetic Ni–Mn–Ga. Appl. Phys. Lett. **77**(6), 886–888 (2000)
24. V. Chernenko, E. Cesari, V. Kokorin, I. Vitenko, The development of new ferromagnetic shape memory alloys in Ni-Mn-Ga system. Scr. Metall. Mater. **33**(8), 1239–1244 (1995)
25. J. Pons, V. Chernenko, R. Santamarta, E. Cesari, Crystal structure of martensitic phases in Ni–Mn–Ga shape memory alloys. Acta Mater. **48**(12), 3027–3038 (2000)
26. Y. Feng, J. Sui, Z. Gao, G. Dong, W. Cai, Microstructure, phase transitions and mechanical properties of Ni50Mn34In16− yCoy alloys. J. Alloys Compd. **476**(1–2), 935–939 (2009)
27. R.Y. Umetsu, X. Xu, R. Kainuma, NiMn-based metamagnetic shape memory alloys. Scr. Mater. **116**, 1–6 (2016)

28. S. Ma, C. Shih, J. Liu, J. Yuan, S. Lee, Y. Lee, H. Chang, W. Chang, Wheel speed-dependent martensitic transformation and magnetocaloric effect in Ni–Co–Mn–Sn ferromagnetic shape memory alloy ribbons. Acta Mater. **90**, 292–302 (2015)
29. M. Kök, S.B. Durğun, E. Özen, Thermal analysis, crystal structure and magnetic properties of Cr-doped Ni–Mn–Sn high-temperature magnetic shape memory alloys. J. Therm. Anal. Calorim. **136**(3), 1147–1152 (2019). https://doi.org/10.1007/s10973-018-7823-5
30. W. Ito, Y. Imano, R. Kainuma, Y. Sutou, K. Oikawa, K. Ishida, Martensitic and magnetic transformation behaviors in Heusler-type NiMnIn and NiCoMnIn metamagnetic shape memory alloys. Metall. Mater. Trans. A **38**(4), 759–766 (2007)
31. J. Sui, X. Zhang, X. Zheng, Z. Yang, W. Cai, X. Tian, Two-way shape memory effect of polycrystalline Ni–Mn–Ga–Gd high-temperature shape memory alloys. Scr. Mater. **68**(9), 679–682 (2013)
32. W. Cai, L. Gao, A. Liu, J. Sui, Z. Gao, Martensitic transformation and mechanical properties of Ni–M-n–Ga–Y ferromagnetic shape memory alloys. Scr. Mater. **57**(7), 659–662 (2007)
33. C. Tan, K. Zhang, X. Tian, W. Cai, Effect of Gd addition on microstructure, martensitic transformation and mechanical properties of Ni50Mn36Sn14 ferromagnetic shape memory alloy. J. Alloys Compd. **692**, 288–293 (2017)
34. L. Wang, H. Xuan, S. Liu, T. Cao, Z. Xie, X. Liang, F. Chen, K. Zhang, L. Feng, P. Han, Enhanced elastocaloric effect and mechanical properties of Gd-doped Ni–Mn–Sn-Gd ferromagnetic shape memory alloys. J. Alloys Compd. **846**, 156313 (2020)
35. R. Coll, J. Saurina, L. Escoda, J. Sunol, Thermal analysis of Mn 50 Ni 50–x (Sn, In) x Heusler shape memory alloys. J. Therm. Anal. Calorim. **134**(2), 1277–1284 (2018)
36. Y. Aydogdu, A. Turabi, A. Aydogdu, M. Kok, Z. Yakinci, H. Karaca, The effects of boron addition on the magnetic and mechanical properties of NiMnSn shape memory alloys. J. Therm. Anal. Calorim. **126**(2), 399–406 (2016)
37. G. Abellán, G.M. Espallargas, G. Lorusso, M. Evangelisti, E. Coronado, Layered gadolinium hydroxides for low-temperature magnetic cooling. Chem. Commun. **51**(75), 14207–14210 (2015)
38. M. Kök, I.N. Qader, S.S. Mohammed, E. Öner, F. Dağdelen, Y. Aydogdu, Thermal stability and some thermodynamics analysis of heat treated quaternary CuAlNiTa shape memory alloy. Mater. Res. Express **7**(1), 015702 (2019). https://doi.org/10.1088/2053-1591/ab5bef
39. I.N. Qader, M. Kok, Z.D. Cirak, The effects of substituting Sn for Ni on the thermal and some other characteristics of NiTiSn shape memory alloys. J. Therm. Anal. Calorim. (2020). https://doi.org/10.1007/s10973-020-09758-w
40. E. Balci, F. Dagdelen, I.N. Qader, M. Kok, Effects of substituting Nb with V on thermal analysis and biocompatibility assessment of quaternary NiTiNbV SMA. Eur. Phys. J. Plus **136**(2), 145 (2021). https://doi.org/10.1140/epjp/s13360-021-01149-w
41. E. Acar, M. Kok, I.N. Qader, Exploring surface oxidation behavior of NiTi–V alloys. Eur. Phys. J. Plus **135**(1), 58 (2020). https://doi.org/10.1140/epjp/s13360-019-00087-y
42. S.S. Mohammed, M. Kok, I.N. Qader, M.S. Kanca, E. Ercan, F. Dağdelen, Y. Aydoğdu, Influence of Ta additive into Cu84−xAl13Ni3 (wt%) shape memory alloy produced by induction melting. Iran. J. Sci. Technol. A **44**(4), 1167–1175 (2020). https://doi.org/10.1007/s40995-020-00909-0
43. C. Tatar, R. Acar, I.N. Qader, Investigation of thermodynamic and microstructural characteristics of NiTiCu shape memory alloys produced by arc-melting method. Eur. Phys. J. Plus **135**(3), 311 (2020). https://doi.org/10.1140/epjp/s13360-020-00288-w
44. F. Dagdelen, E. Balci, I.N. Qader, E. Ozen, M. Kok, M.S. Kanca, S.S. Abdullah, S.S. Mohammed, Influence of the Nb content on the microstructure and phase transformation properties of NiTiNb shape memory alloys. JOM **72**(4), 1664–1672 (2020). https://doi.org/10.1007/s11837-020-04026-6
45. F. Dagdelen, M. Kok, I.N. Qader, Effects of Ta content on thermodynamic properties and transformation temperatures of shape memory NiTi Alloy. Met. Mater. Int. **25**(6), 1420–1427 (2019). https://doi.org/10.1007/s12540-019-00298-z
46. E. Ercan, F. Dagdelen, I.N. Qader, Effect of tantalum contents on transformation temperatures, thermal behaviors and microstructure of CuAlTa HTSMAs. J. Therm. Anal. Calorim. **139**(1), 29–36 (2020). https://doi.org/10.1007/s10973-019-08418-y
47. S.S. Mohammed, M. Kök, Z.D. Çirak, I.N. Qader, F. Dağdelen, H.S.A. Zardawi, The relationship between cobalt amount and oxidation parameters in NiTiCo shape memory alloys. Phys. Met. Metall. **121**(14), 1411–1417 (2020). https://doi.org/10.1134/S0031918X2013013X
48. D. Saini, S. Singh, M. Banerjee, K. Sachdev (eds.) Structural Transformation and Hysteresis Behaviour of Ni46Cu4Mn45Sn5 Alloy Synthesized by Ball Milling Method. Macromolecular Symposia. Wiley Online Library (2017)

49. A. Wederni, M. Ipatov, E. Pineda, J.-J. Suñol, L. Escoda, J.M. González, S. Alleg, M. Khitouni, R. Żuberek, O. Chumak, Magnetic properties, martensitic and magnetostructural transformations of ferromagnetic Ni–Mn–Sn–Cu shape memory alloys. Appl. Phys. A **126**, 1–11 (2020)
50. H. Hedayati, P. Kameli, A.G. Varzaneh, S. Jannati, H. Salamati, Effects of Sn vacancy and excess Sn doping on structural, magnetic and electrical properties of Ni47Mn40Sn13 ferromagnetic shape memory alloy. Intermetallics **82**, 14–19 (2017)
51. J.L.S. Llamazares, A. Quintana-Nedelcos, D. Ríos-Jara, C.F. Sánchez-Valdes, T. García-Fernández, C. García, The effect of low temperature thermal annealing on the magnetic properties of Heusler Ni–Mn–Sn melt-spun ribbons. J. Magn. Magn. Mater. **401**, 38–43 (2016). https://doi.org/10.1016/j.jmmm.2015.10.005
52. Y. Aydogdu, A.S. Turabi, M. Kok, A. Aydogdu, Z.D. Yakinci, M.A. Aksan, M.E. Yakinci, H.E. Karaca, The effect of Sn content on mechanical, magnetization and shape memory behavior in NiMnSn alloys. J. Alloys Compd. **683**, 339–345 (2016). https://doi.org/10.1016/j.jallcom.2016.05.108
53. M. Kök, Z. Yakinci, A. Aydogdu, Y. Aydogdu, Thermal and magnetic properties of Ni 51 Mn 28.5 Ga 195 B magnetic-shape-memory alloy. J. Therm. Anal. Calorim. **115**(1), 555–559 (2014)
54. Y. Aydogdu, A.S. Turabi, M. Kok, A. Aydogdu, H. Tobe, H.E. Karaca, Effects of the substitution of gallium with boron on the physical and mechanical properties of Ni–Mn–Ga shape memory alloys. Appl. Phys. A **117**(4), 2073–2078 (2014)